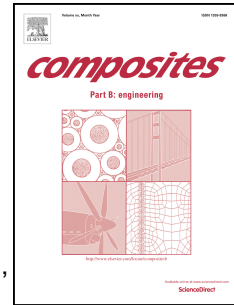# Journal Pre-proof

Towards hemp fabrics for high-performance composites: Influence of weave pattern and features

Anne-Clémence Corbin, Damien Soulat, Manuela Ferreira, Ahmad-Rashed Labanieh, Xavier Gabrion, Pierrick Malécot, Vincent Placet

Please cite this article as: Corbin Anne-Clé, Soulat D, Ferreira M, Labanieh A-R, Gabrion X, Malécot P, Placet V, Towards hemp fabrics for high-performance composites: Influence of weave pattern and features, *Composites Part B* (2019), doi: https://doi.org/10.1016/j.compositesb.2019.107582.

This is a PDF file of an article that has undergone enhancements after acceptance, such as the addition of a cover page and metadata, and formatting for readability, but it is not yet the definitive version of record. This version will undergo additional copyediting, typesetting and review before it is published in its final form, but we are providing this version to give early visibility of the article. Please note that, during the production process, errors may be discovered which could affect the content, and all legal disclaimers that apply to the journal pertain.

Towards hemp fabrics for high-performance composites: influence of weave pattern and features

Abstract: Recent developments in the field of bio-based composite materials are mainly focused on the use of unidirectional reinforcements. The production of woven fabrics and required yarns or rovings is still complex for composite applications due to the finite length of plant fibers and to the high number of process parameters which can be tuned. This study focused on the influence of weave pattern and process parameters on the resulting material properties at different scales. Results from mechanical characterizations and X-ray nanotomography show that very competitive tensile properties can be obtained for woven hemp fabric composites made from low-twisted rovings, in particular when compared to the front-runner flax cross-ply laminate.

1 Introduction

The increase in environmental awareness has stimulated the idea of reducing synthetic-based products in the production of composite materials and more specifically of reinforcements [1]. To achieve this objective of reducing the use of synthetic fibers, the incorporation of cellulosic fibers such as flax, hemp or kenaf has received the attention [2–4]. Indeed, their specific mechanical properties are competitive when compared to glass fibers and they have greater environmental benefits [5–8]. Since the mechanical properties of reinforced composites depend mainly on the nature of the reinforcing fibers, their quantity (fiber volume fraction), their placement and distribution, textile preforms (woven, braided, knitted fabrics, etc.) are widely studied to optimize reinforcement architectures [9,10]. In the textile process, there is direct control over fiber placements and ease of handling of fibers. Textile preforming operations play a key role in most of the composite manufacturing processes. The basic textile yarn and fabric forming processes have been modified and developed to a significant extent to meet the increasing demand from the composite manufacturing sector.

At the scale of the composite material, the best uniaxial mechanical properties are generally obtained when the fibers are aligned in the direction of the applied load [11]. Unfortunately, due to their finite length, it is more difficult to obtain an alignment with plant fibers than with continuous synthetic fibers

[12]. Consequently, many studies on plant fiber composites are related to the development and use of different types of reinforcements (unidirectional (UD), non-woven and woven preforms) [2,13–18]. In these studies, the mechanical properties (bending, impact, tensile) are identified at the scale of composite samples, but also at the fibers' scale using back-calculation method from the mixture law, and/or by the IFBT (Impregnated Fiber Bundle Text) method described in [19]. The use of UD reinforcements is justified by the fact that it is challenging to manage the alignment of reinforcement, at the different scales, in interlacing fabrics when using plant fibers. The main difficulties are associated with the yarn twist, which is necessary in textile technologies to manufacture interlaced fabrics. The twist induces a reduction of the ultimate fiber strength in the final composite by a factor $\cos^2(2\alpha)$ where α is the angle of twist [15,20–22]. It can also restrict the polymer penetration into the reinforcing fiber bundles [23]. For fabric architectures with high crimp, the in-plane mechanical properties (e.g. stiffness and strength in tension and compression) can also be reduced [9]. Another difficulty when using interlaced fabrics is related to the prediction of their properties. The use of modified mixture laws, as proposed by different authors [24,25] and taking into account the degree of alignment, requires the knowledge and measurement of the torsion. However, during the composite manufacturing stages, such as the preforming step [26], the injection molding step [16] or the impregnation according to the viscosity of the matrix [23,27], particularly on complex shapes, the alignment of reinforcement is significantly modified. In addition, the drapability of fabrics on double-curvature molds cannot be achieved with UD preforms, to achieve this goal at least two directions of interlaced (or stitched) reinforcements must be present. So, one of the main advantage of the textile fabrics when compared to the UD tapes is effectively their very good drapability and their capability for complex shape formation with no gap. These elements allow the reduction of the manufacturing costs and times.

The development of interlaced reinforcement architectures based on natural fibers with controlled characteristics is therefore a requirement. This work is first dedicated to the manufacturing of woven fabrics made from hemp rovings for composite applications. A roving consists of a continuous alignment of fibers, parallel to each other and slightly twisted. In this work, rovings were preferred to yarns to manufacture woven fabrics. They have higher linear mass density, a higher number of fibers in cross section, and a lower twist level when compared to yarn. This increases the impregnation capability and they are therefore more suited for composite applications. As explained in previous studies [28–31], a

sufficient tenacity is required for manufacturing preforms, which is not necessarily achieved with this type of yarn. In the textile industry, chemical treatments, mainly mercerization processes, are classically used to improve yarns properties and their weavability [32–34]. Flax fibers are commonly used to manufacture reinforcement with low twisted rovings, which are available in the market and well-studied in the literature [26,29,30,35–37]. However, only few studies focused on composites reinforced by low twisted yarns manufactured with hemp rovings, and in these studies, hemp fibers are comingled or cowrapped with thermoplastic polymers [38–42]. In this paper, woven reinforcements are developed with low twisted rovings made of 100% hemp fibers.

In this study, several characterization steps are performed at different scales (fiber, roving, fabric and composites). The performances of the composites made from these woven fabrics are compared to the ones obtained with a cross-ply flax laminate, considered to be the best plant fiber composite currently available on the market. The influence of the weaving step on the fiber features is also discussed.

2 Materials

2.1 Hemp rovings

The mono-dimensional reinforcement used in this study are hemp rovings supplied by Linificio e Canapificio Nazionale, an Italian Company. The rovings are 100% made of hemp fibers. They have a linear density of 259 Tex, measured according to the standard NF G07-316 [43], and a twist level of 36 turns/m, measured according to the standard NF G07-079 [44]. These rovings were submitted to a chemical treatment classically used in textile industry, called mercerization, to improve their tenacity in view of the weaving [45].

2.2 Woven fabric manufacturing

Woven fabrics were manufactured with the above-mentioned hemp rovings on a manual dobby loom, a Leclerc Weavebird weaving machine. The weaving process used is shuttle weaving. Before the weaving process, several preparations steps are required. The first one, called warping, consists in preparing the warp beam: warp yarns are wound parallel to each other, with the length of the future fabric, around the drum of the warping machine and then they are transferred on the warp beam. The further step is the drawing in: once the warp beam is fixed on the dobby loom, the warp yarns are inserted one by one through the heddles and the weaving reed. The weaving can then begin: the weave pattern is created with the movement of the dobby frames and between to movements, the shuttle is passed inside the shed to

insert the weft yarn and the weaving reed is refolded to compress and form the fabric. Three fabrics with different weaving diagrams were produced, i.e. plain weave (H1), satin 6 weft effect (H2) and twill 6 weft effect, see Figure 1. On schematic views, made with WiseTex software, warp yarns are represented in blue color and weft yarns in red color. They have the same warp density of 6 yarns/cm and different weft densities, namely 5 yarns/cm for H1 and 9.5 yarns/cm for H2 and H3. Warp and weft densities have been measured according to the standard NF ISO 4602 [46].
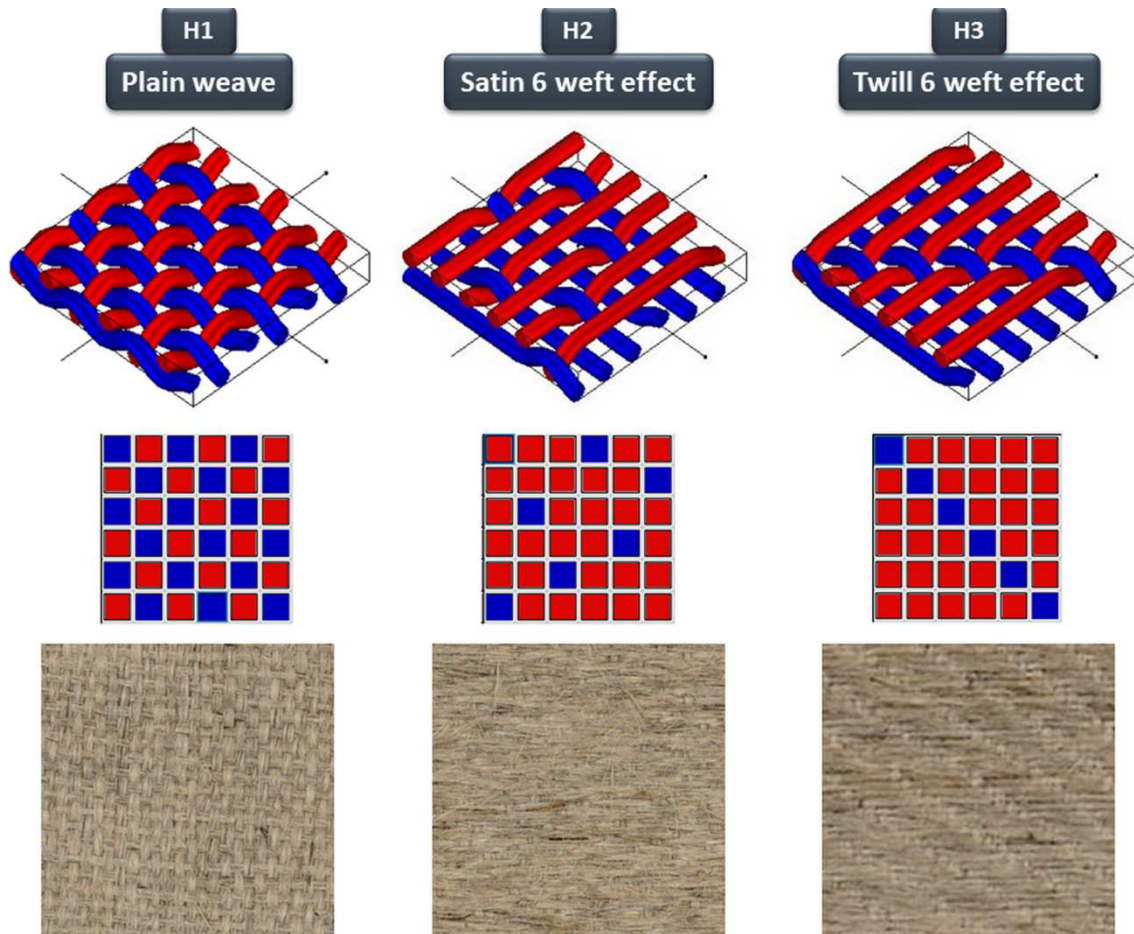

Figure 1: Schematic representation and pictures of the woven fabrics manufactured and studied in this work

2.3   Composite manufacturing

Two types of composites were manufactured: plates and IFBT (Impregnated Fiber Bundle Test) specimens.

Composites plates were manufactured by hot pressing with the produced hemp fabrics and an epoxy resin, the GreenPoxy 56 from Sicomin Company. Their dimensions are 200 x 300 mm². The fabrics were conditioned at a temperature of 23°C and a relative humidity of 50% during at least 24 h prior to the

composite manufacturing. After this pre-conditioning, the plies were hand layed-up, impregnated manually with the epoxy resin and then cured at 130°C under a pressure of 3 bars during 1 h. A hot-press Agila Press 100 kN was used. As there are three types of fabrics, three types of composites were manufactured (noted as C1, C2 and C3 with the H1, H2 and H3 reinforcements, respectively). Four plies were stacked for C1 and C2 composites and two plies for C3. All the plies were stacked with the same orientation. During composite manufacturing, there is 1.6 times the mass of resin compared to the mass of fibers. The mold is open at the ends, which allows the excess resin to be removed. Following the manufacturing, the composite plates were conditioned at 23°C and 50% RH during at least four weeks to reach the moisture content equilibrium. In order to compare the properties of the composites reinforced by the woven fabrics, a "reference" composite was also manufactured with a pure unidirectional flax reinforcement. The FlaxTape^{TM} 110 by Lineo Company was used to manufacture a cross-ply laminate with the same protocol.

IFBT specimens were also prepared by aligning the hemp rovings and impregnating them with GreenPoxy 56 resin. After impregnation, the specimens were cured at 60°C during 24 under a pressure of 2 bars. The dimension of the manufactured specimens are approximately 200 mm x17 mm x 1 mm. Prior to the manufacturing of the IFBT specimens, the hemp rovings were conditioned at a temperature of 23°C and a relative humidity of 50% during few hours to reach the equilibrium. After manufacturing, the IFBT specimens were also stored in a climatic chamber (23°C - 50% RH) during a minimum of three weeks to reach the moisture content equilibrium.

For both composite plates and IFBT specimens, the quantity of resin was calculated to reach a fiber volume fraction in composites of approximately 40%. The real fraction of each specimen and each plate was measured after manufacturing.

3   Characterization methods

3.1   *Fiber properties - Impregnated Fiber Bundle Test (IFBT)*

The IFBT test was used to determine by inverse method the effective tensile properties of the hemp fibers constituting the rovings. In this method, fully described in [19], rovings are aligned in the same direction and impregnated with the resin to manufacture composite samples. Tensile tests are then done on these samples, and the effective modulus of fibers is obtained by back-calculation using a rule of mixtures. In this work, we used the following law [21,22,24,25,45,47,48], fully described by Eqs. 1-3:

$$E_c = (\eta_0 \eta_1 V_f E_f + V_m E_m)(1 - V_p)^n \tag{1}$$

$$\eta_0 = \cos^2(2\alpha) \tag{2}$$

$$\alpha = \tan^{-1}(2\pi r T) \tag{3}$$

where E_C is the composite modulus, η_0 a fiber orientation factor, η_1 the fiber length factor, V_f the fiber volume fraction, V_m the matrix volume fraction, V_p the porosity volume fraction, E_f is the fiber modulus (in the longitudinal direction), E_m the matrix modulus, n the porosity factor, α the surface twist angle, r the radius of roving and T the twist level of roving.

Taking into account the non-linear tensile behavior generally observed for plant fiber composites, and for comparative purpose, the composite modulus was measured on two different strain ranges: E_{1C} between 0 and 0.1% of longitudinal strain and E_{2C} between 0.3 and 0.5%. The corresponding modulus determined by back-calculation at the scale of the fibers were noted E_{f1} and E_{f2}. The fiber length factor (η_1) was considered equal to 1 (which is generally the case when the length to diameter ratio of the fibers is higher than 50). Based on the empirical results reported in literature [22,48], the porosity factor (n) was considered equal to 2.

Tensile tests were conducted on five IFBT specimens using a MTS Criterion 45 universal machine, with a crosshead displacement rate of 1 mm/min. The longitudinal strain was measured with an Instron 2620-601 extensometer with a gauge length of 50 mm.

3.2 Roving properties

At the roving scale, the twist level was studied according to the standard NF G07-079 [44] on 10 samples per type of yarn. The tenacity was measured using tensile tests. For each yarns, 10 specimens were tested using a MTS Criterion 45 tensile machine, with a load cell of 10 kN, a gauge length of 200 mm, a crosshead displacement rate of 200 mm/min and a preload of 0.5 cN/Tex, according to the standard NF EN ISO 2062 [49].

The same properties were also determined after weaving to evaluate the influence of the weaving process on these features. The rovings were manually extracted from the fabrics.

3.3 Fabric properties

The areal density and the thickness of the different fabrics were measured on 10 specimens according to the standards NF EN 12127 [50] and NF EN ISO 5084 [51], respectively.

Compaction tests were also performed on woven fabrics, on three specimens for each fabric, to characterize and compare the compressibility behavior of the different weave patterns and to determine the fiber volume fraction as a function of applied pressure. This is an important parameter for the composite manufacturing processes. The compaction tests were performed on a MTS Criterion 45 universal machine with a full-range load cell of 100 kN at a crosshead displacement rate of 1 mm/min. The pressure was applied with a compaction cylinder with a diameter of 62.5 mm until a pressure of 20 MPa. The displacement was measured with a LVDT sensor, mounted between the compaction cylinder and the bottom plate, with a full range of 2.5 mm and an accuracy of 2.5 µm. The compressive frame stiffness of the test set-up was also measured and taken into account to correct the measured displacement, as suggested in [52–54]. Square samples of the fabrics with dimensions of approximately 80x80 mm² were laid-up in the same material direction (see Figure 3). For all the tests, four plies were used. The initial thickness of the lay-ups was measured on the machine with a pre-load of 10 N. Three successive loading/unloading steps were then applied. Only the first loading is analyzed in this study. The pressure is calculated by dividing the applied force by the area of the compaction cylinder, and the strain by dividing the measured displacement by the initial thickness.
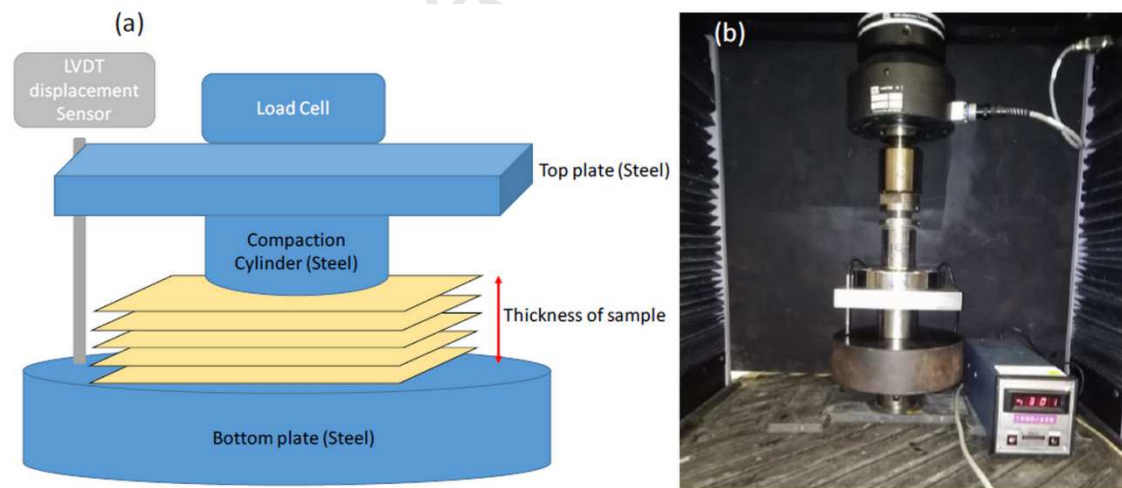

Figure 2: Compaction test setup a. schematic diagram with preforms b. configuration for machine stiffness measurement
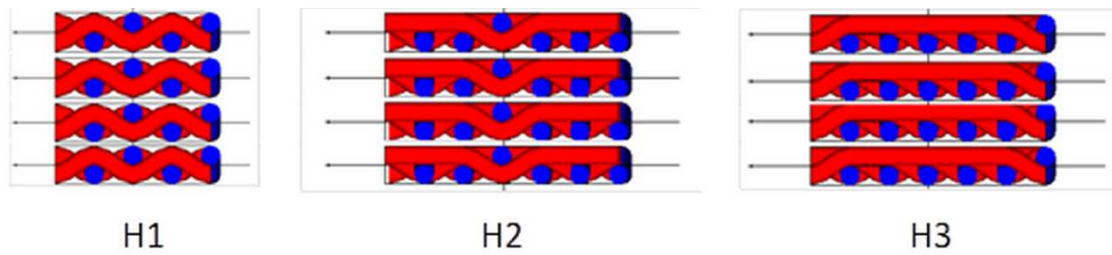
Figure 3: Schematic view of the stacking sequence in compaction tests (weft direction in red, warp direction in blue)

3.4 Composite properties

The microstructure of the manufactured composites was characterized using X-ray nanotomography. Image acquisition was realized on an Easytom micro-nano tomograph (RX Solutions, France). The system is equipped with an X-ray source Hamamatsu Open Type Microfocus L10711 having maximum voltage 160 keV. The images reported herein were collected using X-rays of voltage 40 keV and a current of 22 µA. The X-ray transmission images were acquired using a Fluoroscopic High Speed imaging sub-system PaxScan 2520DX. The entire volume is reconstructed at a full resolution with a voxel size of 5.77 µm, using filtered back-projection. The data were processed using VG Studio software.

Tensile specimens were cut in the manufactured composite plates using a Trotec laser cutter. The mechanical characterization was conducted according the standard ASTM D3039-00 [55], on a MTS Criterion 45 universal machine, with a crosshead displacement rate of 1 mm/min, a specimen width of 15 mm and a gauge length of 150 mm. For samples per direction (warp and weft) are tested for all the composites materials. The longitudinal strain was measured with an Instron 2620-601 extensometer with a gauge length of 50 mm.

4 Results and discussions

4.1 Influence of weave pattern on the fabric properties

The textile properties measured on the woven fabrics are presented in Figure 4.a.for the areal density and in Figure 4.b. for the thickness and weft density. H2 and H3 fabrics have a similar areal density of approximately 400 g.m^{-2}, which is approximately 1.4 times higher than the one of H1. This can be explained by the interlacement and the weft density. Indeed, the H2 and H3 fabrics, which are satin 6 and twill 6 weave patterns, have one binding point for 6 rovings, whereas the H1 fabric (plain weave pattern) has one binding point for two rovings. A binding point is the interlacement between warp and weft

rovings, represented by black squares in Figure 1. Thus, as rovings are less interlaced in H2 and H3 fabrics, they are more compacted on top of each other and the weft density is higher. As a result, there are more rovings per unit area in H2 and H3 fabrics, and the areal density is higher than for H1 fabric.
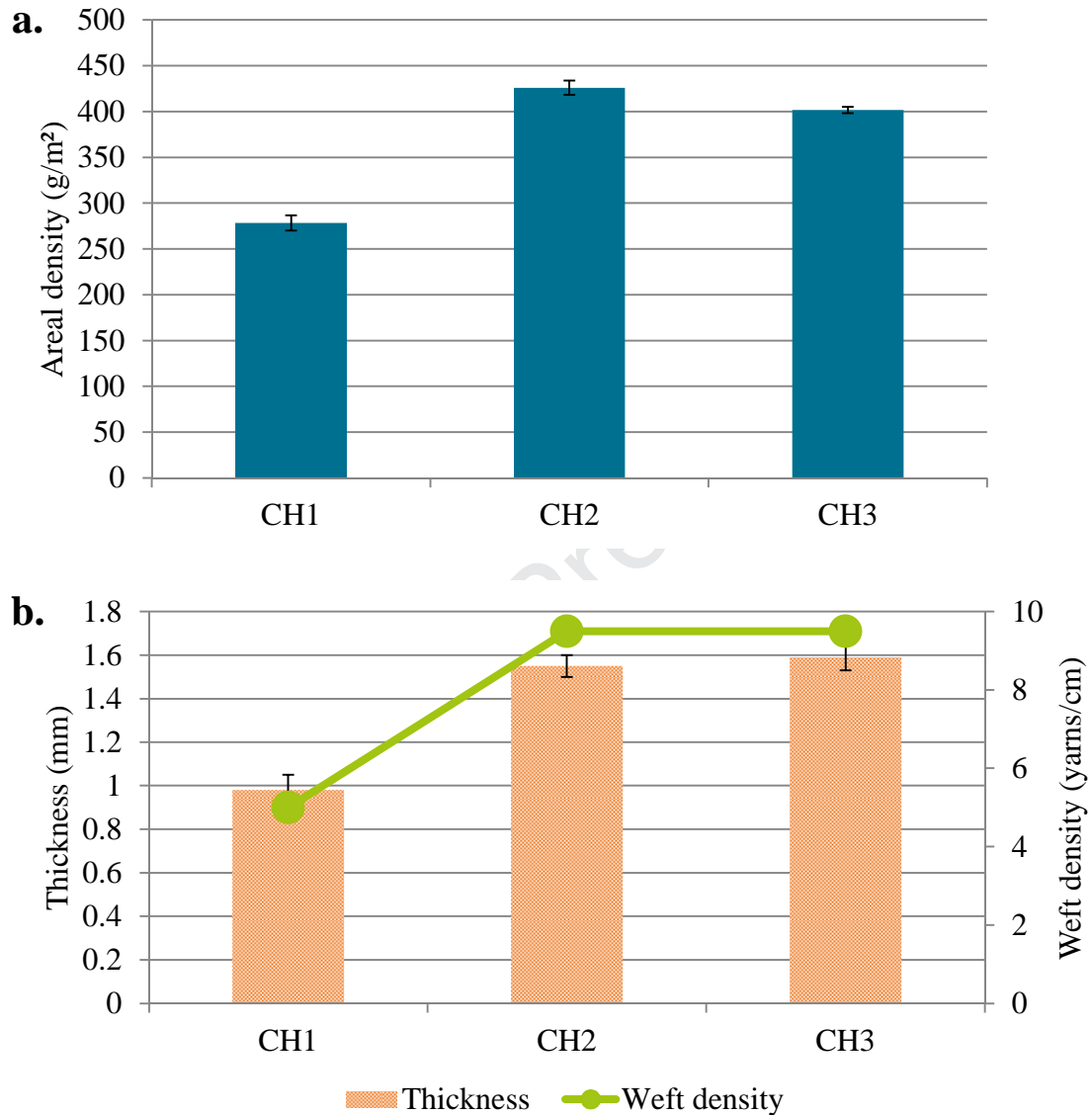

Figure 4: Properties of the woven fabrics a. Areal density b. Thickness and weft density

The compressibility of the different fabrics was also characterized. The compaction curves are shown in Figure 5. The three fabrics exhibit a very similar behavior with a maximum fiber volume fraction of approximately 70%. In this way, it can be expected that the composite made with these three fabrics will have similar fiber volume fraction after manufacturing steps.

The compaction response is strongly non-linear (see Figure 5). As explained by different authors [56,57] this results from the expression of different phenomena. In the first stage, for low pressure, the

9

response is quasi-linear. It results from the combination of the deformation of the roving cross-section, the roving flattening and nesting. In the second stage, the curve becomes nonlinear and in addition to the first mechanisms, the bending of the roving takes place, which leads to the reduction of void and slippage between fiber and/or roving. At last, a third phase, linear again, is observed. The compaction is then attributed to the transverse compression of fibers
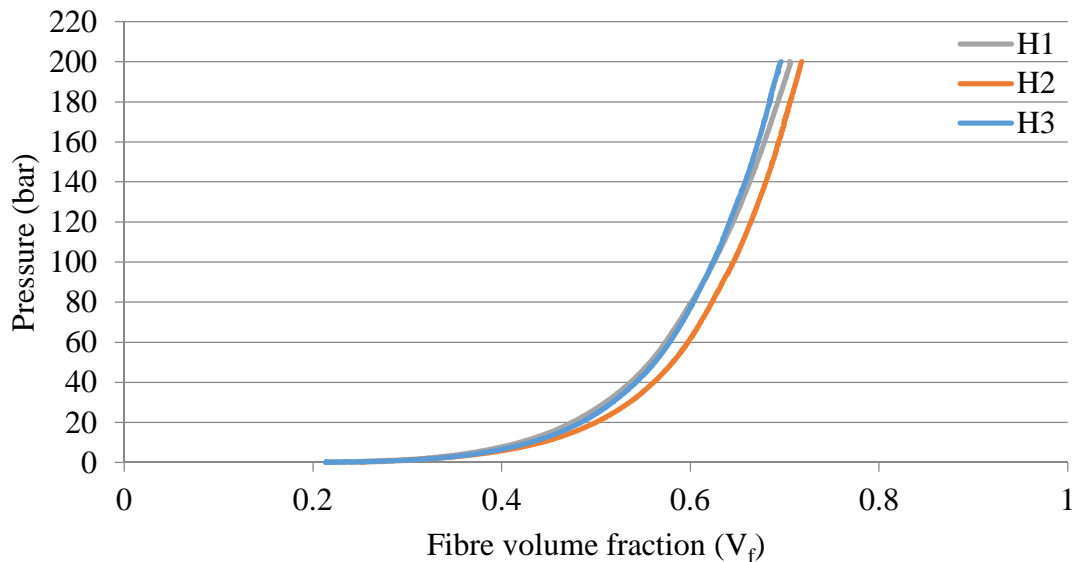

Figure 5: Compaction curves for the three hemp fabrics

4.2   *Influence of the weaving process on the roving features and fiber orientation*

During the weaving process, the roving properties are impacted. The values of the twist level and of the breaking tenacity of rovings before and after weaving for each fabric are shown in Figure 6.a and Figure 6.b, respectively. In the warp direction, the values of twist level remains in the standard deviation whereas in the weft direction, the twist level decreases significantly after weaving. This untwisting is more important for the weft rovings inside H2 than in H3 and H1 fabrics. A decrease of approximately 94% in the twist level is measured for the roving from the H2 fabrics against a decrease of 61% for the roving from H3 fabric and 51% for the roving from H1 fabric. This trend is similar for the decrease of breaking tenacity, always in weft direction: there is a decrease of approximately 46% for H2 fabric, 34% for H3 fabric and 16% for H1 fabric. This is consistent with the decrease in twist level. When the rovings are less twisted there is less cohesion between fibers and then the strength is reduced. The decrease in the twist level of weft rovings is attributed to the technique used for the weft insertion in shuttle weaving.

Whereby, the weft rovings need to be wound into a small bobbin, called a quill, which is inserted in the shuttle to pass the weft roving through the shed.

In the warp direction, even if the standard deviations are quite high, an increase of tenacity at break after weaving can be observed. This increase is more important for the H2 fabric. For the satin weave pattern, the movement of frames moves rovings which are distant from each other, whereas for plain weave and twill weave patterns, rovings are raised side by side. Indeed, there are less fibers hanging between the warp rovings during the satin weaving process, and they are less "damaged" in the process, which is why they have the best tenacity at break. The warping process and the tension applied on the rovings during the weaving process can stiffen the warp rovings, and confer to them better mechanical properties, especially a better tenacity at break, which is more or less damaged by hanging due to the movement of the frames.
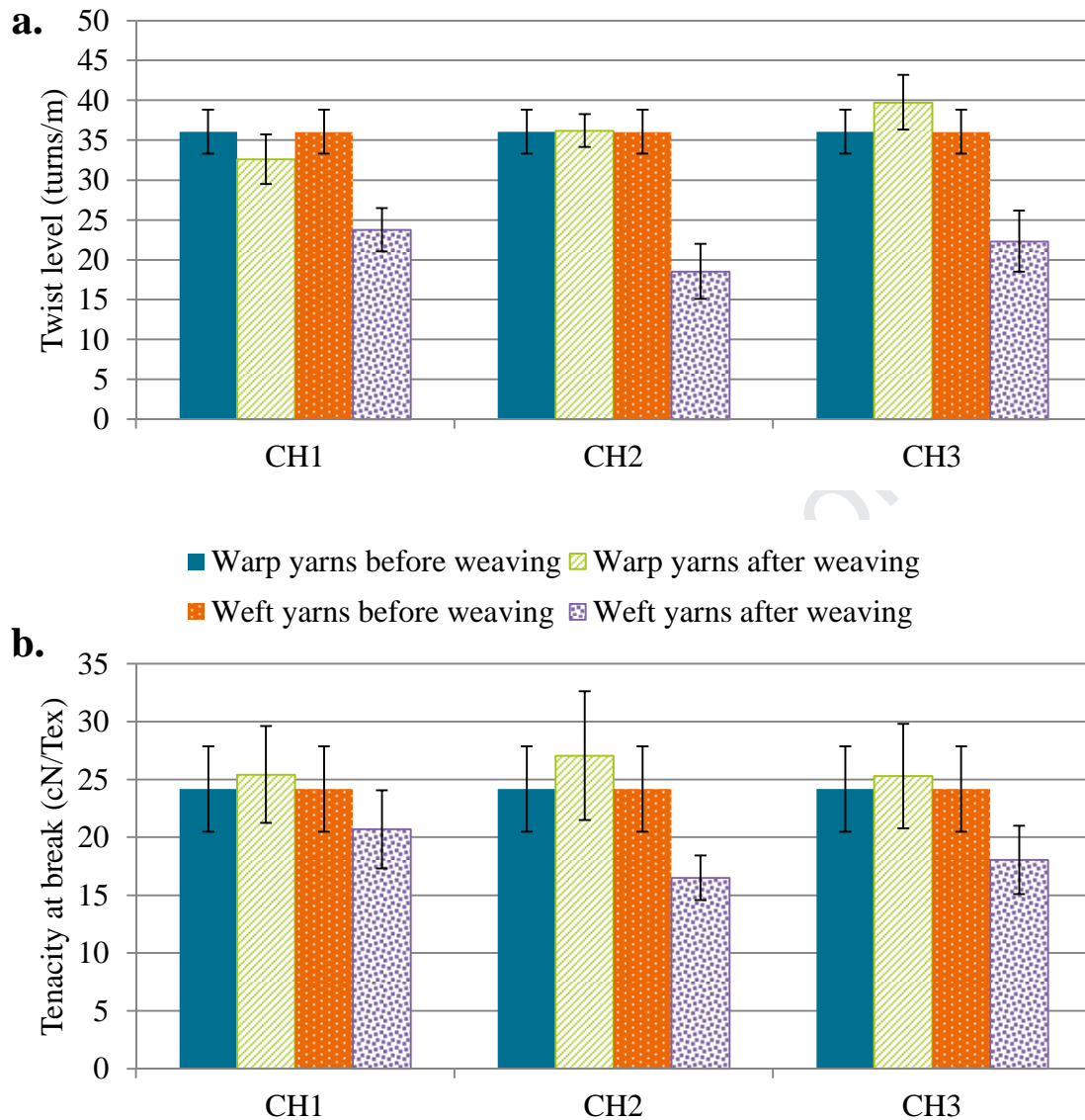
11

a.

b.

Figure 6 : Influence of weaving process on yarns properties a. Twist level b. Tenacity at break

The values of the twist level and tenacity at break before and after weaving are summarized, in Figure 7, to highlight the influence of twist level on tenacity at break. As mentioned in the literature [28,30], the increase in the twist level leads to an increase in the breaking tenacity. The twist level gives more cohesion between the fibers and thus more strength to the rovings.
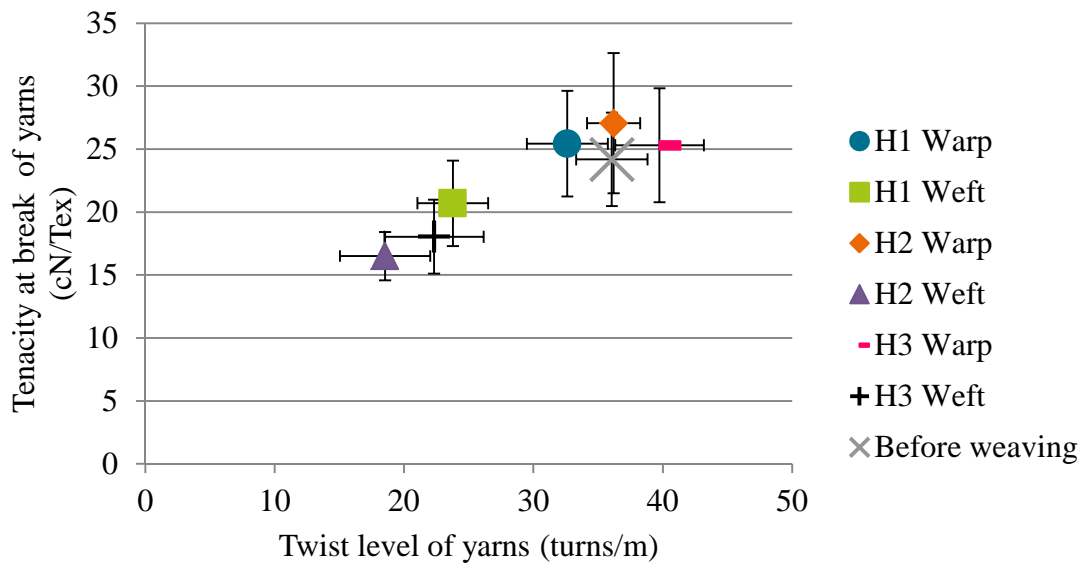
Figure 7: Breaking tenacity of the rovings as a function of their twist level. Evidence of a direct

relationship

The tensile properties of the fibers were also determined before and after weaving using IFBT tests (Figure 8). Before weaving, the rovings were extracted from the bobbins, and after weaving, the rovings are extracted in warp and weft direction from the fabrics. Figure 8 shows the values of the fiber moduli (E_{f1} and E_{f2}) before and after weaving for the three fabrics. These results show the high rigidity of the hemp fibers used for this work, with an initial apparent rigidity (E_{f1}) greater than 60 GPa.

In the weft direction, the fiber modulus E_{f1} after weaving is slightly lower than the one before weaving for the H1 and H3 fabrics. This apparent stiffness reduction could be both attributed to the remaining crimp in the rovings (and the resulting fiber disorientation, neglected when back-calculating the fiber properties) as well as fiber damage induced by the weaving process. Interestingly, the mean E_{f1} value for the H2 fabric is higher after weaving. This improvement of the fiber stiffness can be attributed to a stiffening effect [58] induced by the mechanical loading applied during the weaving process. This effect could counterbalance the potential decrease in fiber stiffness due to their misorientation (remaining crimp effect) and hypothetic damage induced by the weaving. All these underlying mechanisms and microstructural features deserve to be thoroughly studied in forthcoming studies. In the warp direction, the fiber stiffness is more negatively impacted by the weaving process. A decrease of approximately 30% is observed after weaving for the H1 and H3 fabrics. Again, this effect is less pronounced for the H2 fabric. As a conclusion, it can be underlined that the fiber stiffness is well preserved during the processing

of the satin fabric, and even improved for the fibers oriented in the weft direction. All the results above-mentioned are also valid for E_{f2}.
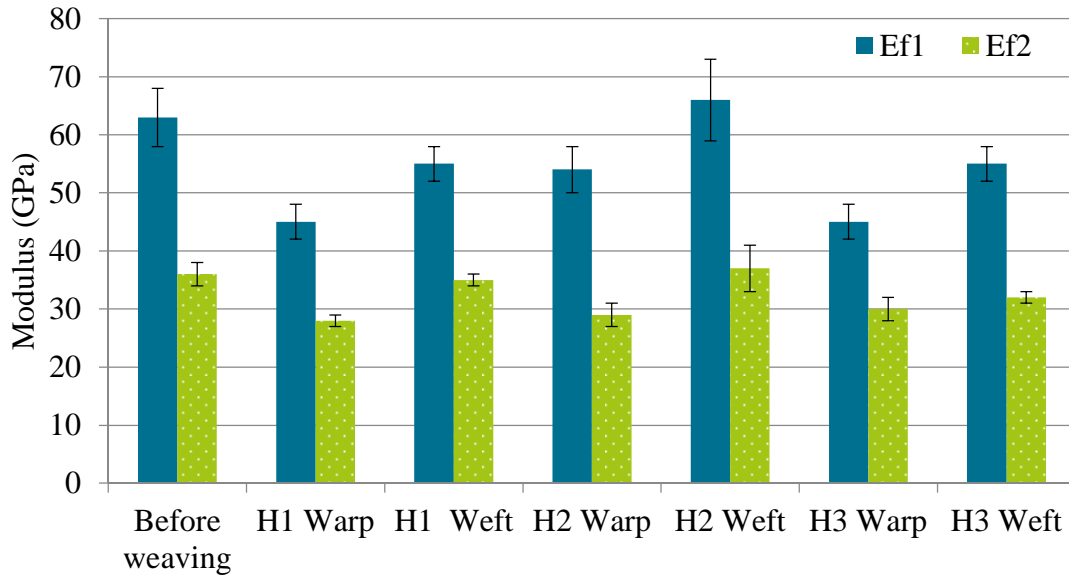

Figure 8: Comparison of the fiber stiffness before and after weaving for the three considered fabrics

4.3 *Influence of the weave pattern on the composite properties*

Using these three fabrics (H1, H2 and H3), composite materials were manufactured, respectively noted CH1, CH2 and CH3. The thickness and the microstructural features are shown in Table 1. Two methods were used to determine the constituent volume fractions. The first one is by weighting, as described in [59]. The second one is by using X-ray nanotomography images analysis and reconstruction.

Table 1: Composites composition and thickness

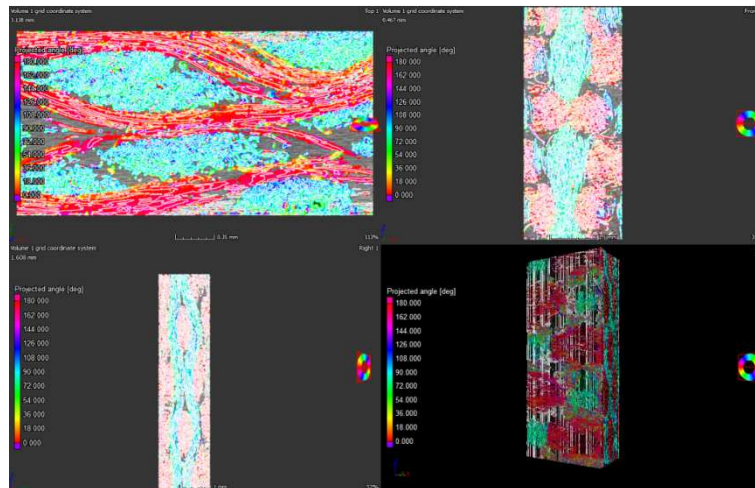| Composites	Weave pattern	Thickness (mm)	Weight calculation		Nanotomography	
			V_f (%)	V_p (%)	V_f (%)	V_p (%)
CH1	Plain weave	1.70 ± 0.04	42.4	2.4	43.0	0.8
CH2	Satin	2.46 ± 0.05	46.0	0.4	48.8	1.5
CH3	Twill	1.42 ± 0.06	37.0	3.0	41.0	1.1

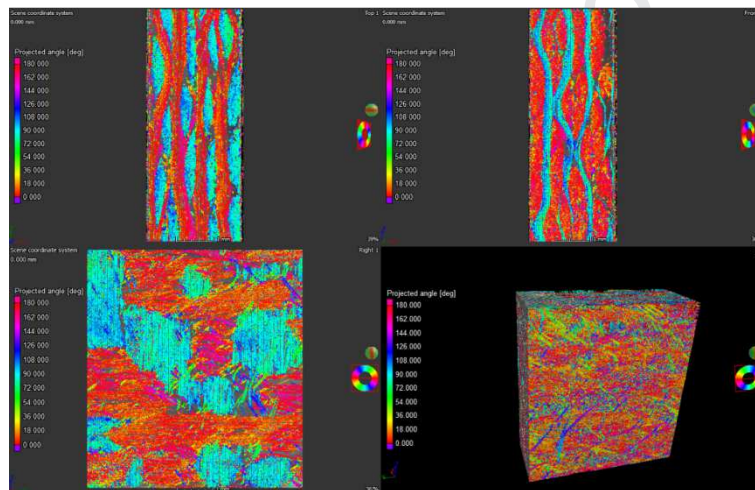*Figure 9: Nanotomography views of CH1 composite*

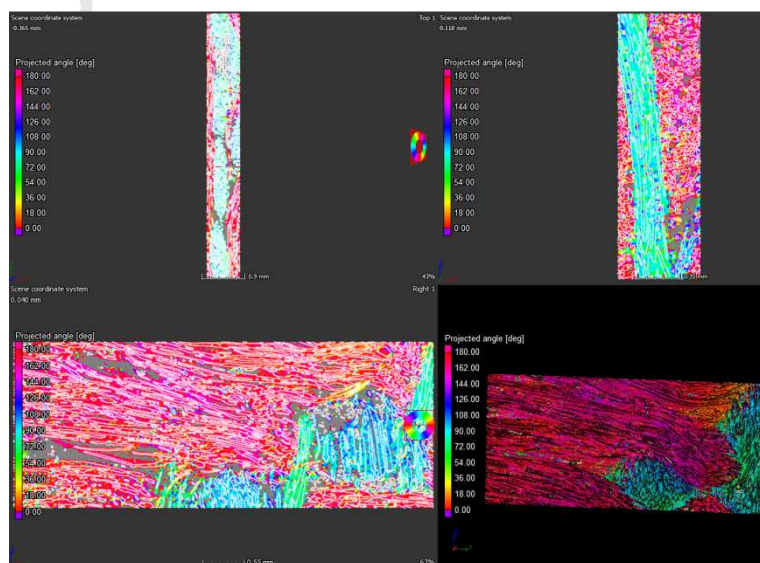*Figure 10: Nanotomography views of CH2 composite*

Figure 11: Nanotomography views of CH3 composite

In order to conduct observations inside the composite materials, nanotomography imaging is used. Some images are presented in Figure 9, Figure 10 and Figure 11, respectively for CH1, CH2 and CH3 composites. For the three composites, some porosity can be observed, which is mainly located between the plies but also inside the rovings. However, there is not a lot of porosity, and none of the composites have major impregnation defects. The process used is thus suitable for the manufacture of the composite plates. With nanotomography analysis, it is also possible to study the distribution of porosities throughout the thickness of the composite samples (see Figure 12). For CH1 and CH2, porosities are evenly distributed over all plies whereas for CH3, porosities are more located in the upper ply (as a reminder, CH3 is made of only two plies).
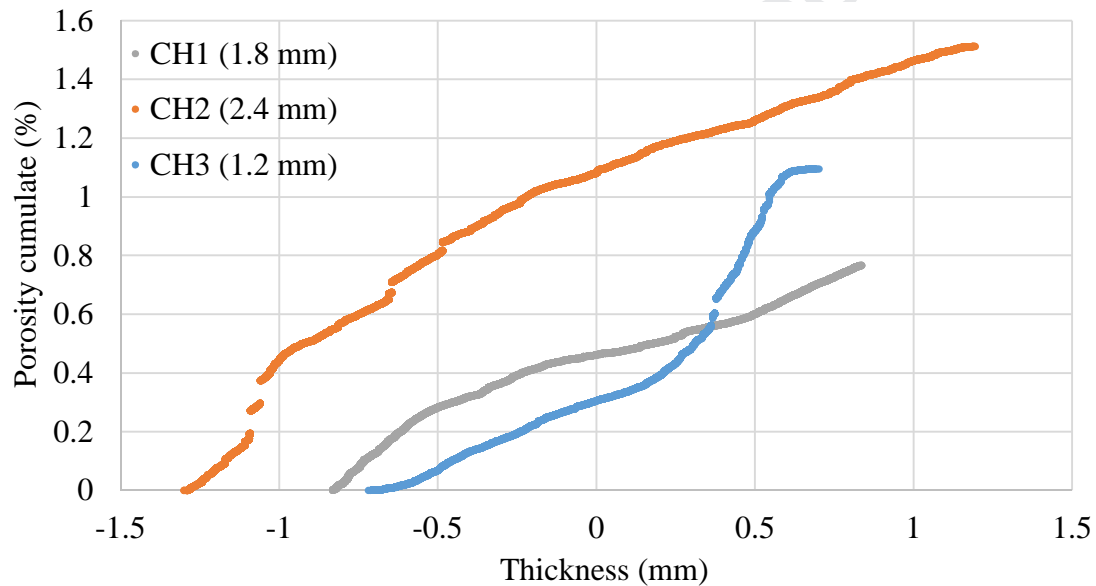

Figure 12: Distribution of porosities through the thickness of the composite samples

The mechanical properties of the three composites are presented in Figure 13.a. for the modulus and in Figure 13.b for the strength. Since the fiber volume fraction was slightly different for each composite type, and to facilitate the comparison, the properties were normalized with a fiber volume fraction of 45%, using a rule of mixture. It can be observed that the satin weave pattern leads, at the scale of the composite material, to the best mechanical properties in the weft direction. In the weft direction, the modulus is 10% higher than in the warp direction for CH1, 44% higher for CH2 and 31% higher for CH3. For the strength at failure, the value in the weft direction is 20% higher than in the warp direction for CH1, 49% for CH2 and 41% for CH3. Indeed properties are more similar between the warp and weft direction in CH1 composite than in the CH2 and CH3 composites. As expected, the plain weave pattern

16

gives the better balanced properties to its composite. In the H2 and H3 fabrics, the weft density is higher than in the H1 fabric due to the weave pattern, there are also more fibers in this direction, and the resulting mechanical properties are higher in the weft direction. Moreover, in the weft direction, the rovings are untwisted during the weaving process, as shown previously in Figure 6.a., and thus the fibers are more aligned with the loading direction. In this way, the mechanical properties are higher in the weft direction than in the warp direction, thanks to a higher fiber volume fraction and a better alignment of the fibers in the direction of the mechanical stress.

The mechanical properties of these composites (CH1, CH2 and CH3) made from a woven fabric were also compared to the one obtained for a cross-ply laminate stacking sequence, consisting of 0° and 90° purely unidirectional flax fiber plies. In terms of mechanical properties, the composite reinforced by unidirectional plies has a tensile strength of 182 MPa and a modulus of 18.7GPa in both directions. In comparison with the reference composite, the modulus in the warp direction of each woven composite is lower (-23% for CH1, -40% for CH2 and CH3) but quite similar or higher in the weft direction (-14% for CH1, -7% for CH2 and -12% for CH3). This trend is similar for the strength at failure: the values in the warp direction are lower than for the reference composite (-30% for CH1, -47% for CH2 and -46% for CH3) and similar higher in the weft direction (-3% for CH1, 17% for CH2 and 5% for CH3). By using a plain weave pattern for woven fabric reinforcement, the properties obtained are closer than those which can be achieved with a symmetrical cross-ply laminate. The use of a more complex weave pattern, such as satin or twill, leads to more unbalanced properties, but which can be higher in one direction than those of a composite manufactured with unidirectional plies. These results are consistent with what had already been demonstrated in another study with hemp/PLA comingled rovings, in which composite reinforced by satin woven fabric has higher properties than the one reinforced by basket woven fabric [41].Thus, it can be assumed than these results are promising, and high performance composites can also be manufactured with woven fabrics made of 100% hemp low twisted rovings as reinforcements.
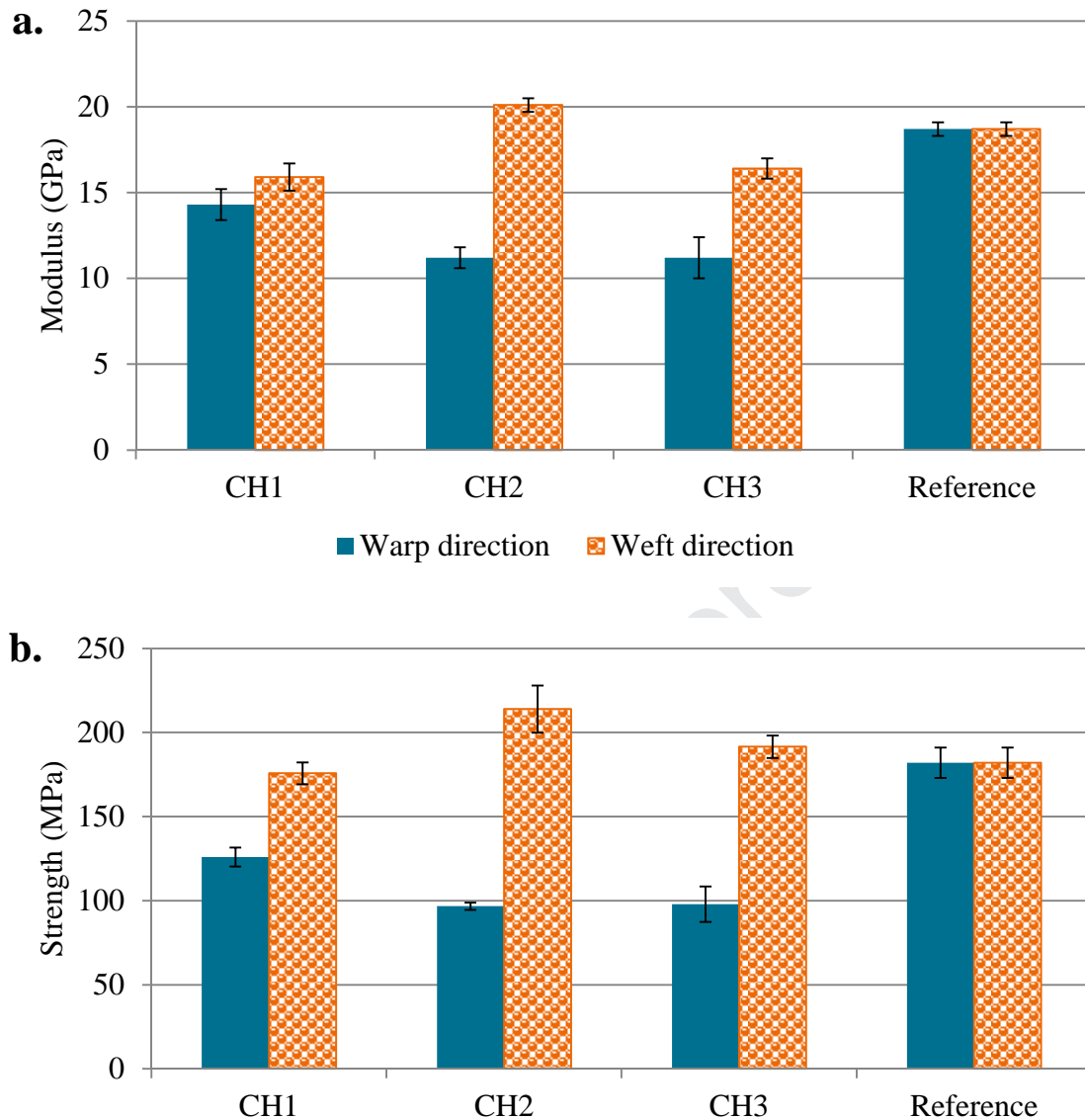
Figure 13: Composite mechanical properties estimated at $V_f = 45\%$ (Reference = flax cross-ply laminate)

a. Modulus b. Strength

4.4   Influence of rovings features on composite properties

As seen previously, the roving properties are influenced by the weaving process. The main parameter altered by the weaving process is the twist level. This factor is really influential on the fiber alignment in composite materials and thus on the mechanical properties which result at the scale of the composite material.

Table 2: Percentage of fibers in composite in two main material directions

Composite	Warp direction (%)	Weft direction (%)	Total (%)

CH1	47	47	94
CH2	40	51	91
CH3	42.5	47.5	90

The percentage of fibers in the two main directions was determined from the tomography analysis. The values are determined from a single sample for each composite and shown in Table 2. The total percentage of fibers in warp and weft directions is lower than 100% due to misalignments of fibers mainly due to twisting of rovings. By twisting the rovings, fibers are positioned in other directions than the main direction of the rovings, and thus, after weaving, they are oriented in other directions than the warp or weft direction of the fabrics. In this way, the twist level of rovings after weaving (Figure 6.a.) was compared with the percentage of fibers in the main directions of the composite (Table 2). It can be conclude that the more the twist level of rovings after weaving is decreased during the weaving process, the higher is the fiber content in the composite direction. By decreasing the twist level of the roving during weaving process, the fibers are more aligned in the direction of the mechanical stress.

By plotting the strength of the composites measured in both material directions for the different woven fabrics according to the twist level of the rovings (measured after weaving), we confirm a direct relationship already mentioned in the literature: the more the fibers are aligned in the roving main axis and the load direction, the higher the strength of the composite[21,28,30].
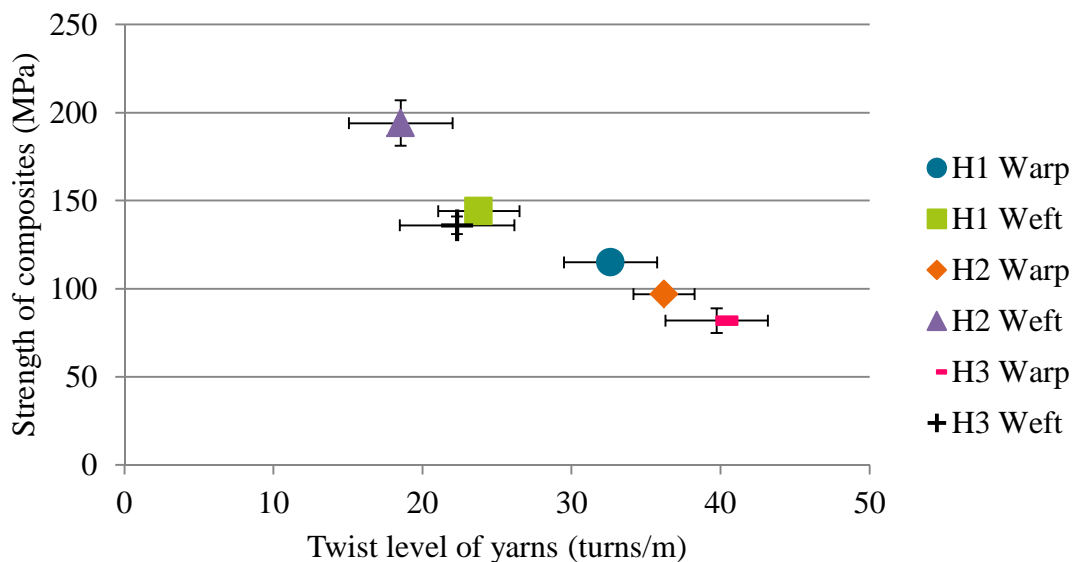

Figure 14: Relationship between the twist level of the rovings in the fabrics and the strength of

composites

The properties of the composites were also predicted using a V_f equal to 45%, the rule of mixtures, and the back-calculated properties of the fibers, their twist level in the rovings and the properties of the matrix. The results are presented in Figure 15. The rule of mixture used is presented in Eqs. 1-3. In ROM1, the values of the fiber modulus and the twist level correspond to the ones measured before weaving, whereas in ROM2, the values after weaving are considered. The moduli of fibers E_{f2} before and after weaving used are the ones presented in Figure 8. The composite properties obtained using ROM1 are clearly under- or overestimated for all materials: approximately 10% of difference between experimental and predicted values in both directions. However, by using the fiber and roving properties after weaving, the composite properties are predicted with a better agreement when compared to experimental data (the relative difference between experimental and predicted values varies from 1% to 6%) excepted for warp direction in CH1 and CH3 composites (respectively 36% and 24% of difference between experimental and predicted values). To obtain a good prediction, the fiber and roving properties after processing have to be considered. One of the remaining questions is the influence of the composite manufacturing (in particular pressure and temperature) on the fiber and roving features. This will be studied in a further step using the X-ray nanotomography results.
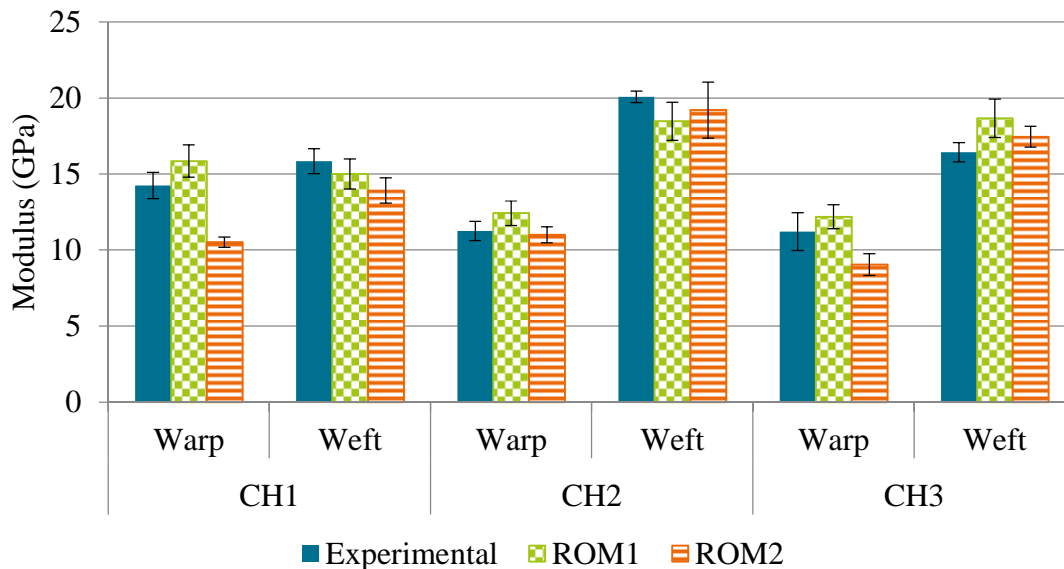

Figure 15: Comparison of experimental modulus and predicted modulus of composites

5   Conclusion

Woven fabrics are used to manufacture composite materials with advanced properties because they are more deformable without defects, which allows for better handling during the manufacturing process, and

they can endure higher in-plane shear stress, in comparison with unidirectional reinforcements. In this study, the influence of weaving process parameters, and especially the weave pattern, has been studied at different scales. Compaction tests have also been conducted on woven fabrics and do not highlight significant differences between the weave patterns, thus the fiber volume in the final composite can be expected to be similar for the three materials. Afterwards, the influence of weaving process on rovings and fibers properties has been studied. Due to the untwisting of rovings used in weft direction during weaving process, cohesion between fibers in the cross section becomes less important, which reduces the tenacity at break of the rovings. Despite this untwisting of the rovings, after weaving, the effective stiffness of fiber (studied through IFBT method) is decreased in most cases. This effect is lower when weaving a satin pattern. A fiber stiffening is even observed in the weft direction. Whatever the weave pattern used, only few pores can be observed in composites through tomography analysis. Regarding the mechanical properties of the composites, the use of several weave diagrams leads to balanced or unbalanced properties between the two main directions, depending on the yarn density and the fiber fraction in the studied direction. The percentage of fibers aligned in the direction of the mechanical stress was directly linked to the untwisting of the rovings in this direction during the weaving process. The determination of the effective fiber properties after weaving allows also better composite properties prediction through the rule of mixtures. Results at the scale of composite highlights that mechanical properties similar to the best flax cross-ply laminates can be achieved with hemp woven fabrics made from low-twisted rovings.

Acknowledgements

References

[1] Dhar Malingam S, Lin Feng N, Akmar Kamarolzaman A, Tzy Yi H, Ab Ghani AF. Mechanical Characterisation of Woven Kenaf Fabric as Reinforcement for Composite Materials. Journal of Natural Fibers 2019:1–11. https://doi.org/10.1080/15440478.2019.1642827.
[2] Gourier C, Bourmaud A, Le Duigou A, Baley C. Influence of PA11 and PP thermoplastic polymers on recycling stability of unidirectional flax fibre reinforced biocomposites. Polymer Degradation and Stability 2017;136:1–9. https://doi.org/10.1016/j.polymdegradstab.2016.12.003.

[3]   Bourmaud A, Beaugrand J, Shah DU, Placet V, Baley C. Towards the design of high-performance plant fibre composites. Progress in Materials Science 2018;97:347–408. https://doi.org/10.1016/j.pmatsci.2018.05.005.

[4]   Del Masto A, Trivaudey F, Guicheret-Retel V, Placet V, Boubakar L. Investigation of the possible origins of the differences in mechanical properties of hemp and flax fibres: A numerical study based on sensitivity analysis. Composites Part A: Applied Science and Manufacturing 2019;124:105488. https://doi.org/10.1016/j.compositesa.2019.105488.

[5]   Faruk O, Bledzki AK, Fink H-P, Sain M. Biocomposites reinforced with natural fibers: 2000–2010. Progress in Polymer Science 2012;37:1552–96. https://doi.org/10.1016/j.progpolymsci.2012.04.003.

[6]   Gurunathan T, Mohanty S, Nayak SK. A review of the recent developments in biocomposites based on natural fibres and their application perspectives. Composites Part A: Applied Science and Manufacturing 2015;77:1–25. https://doi.org/10.1016/j.compositesa.2015.06.007.

[7]   Martínez P, Garraín D, Vidal R. LCA of biocomposites versus conventional products, Zurich: 2007.

[8]   Bachmann J, Hidalgo C, Bricout S. Environmental analysis of innovative sustainable composites with potential use in aviation sector—A life cycle assessment review. Sci China Technol Sci 2017;60:1301–17. https://doi.org/10.1007/s11431-016-9094-y.

[9]   Katnam KB, Dalfi H, Potluri P. Towards balancing in-plane mechanical properties and impact damage tolerance of composite laminates using quasi-UD woven fabrics with hybrid warp yarns. Composite Structures 2019;225:111083. https://doi.org/10.1016/j.compstruct.2019.111083.

[10] Mouritz AP, Bannister MK, Falzon PJ, Leong KH. Review of applications for advanced three-dimensional fibre textile composites. Composites Part A: Applied Science and Manufacturing 1999;30:1445–61. https://doi.org/10.1016/S1359-835X(99)00034-2.

[11] Swolfs Y, Verpoest I, Gorbatikh L. Recent advances in fibre-hybrid composites: materials selection, opportunities and applications. International Materials Reviews 2019;64:181–215. https://doi.org/10.1080/09506608.2018.1467365.

[12] Pickering KL, Efendy MGA, Le TM. A review of recent developments in natural fibre composites and their mechanical performance. Composites Part A: Applied Science and Manufacturing 2016;83:98–112. https://doi.org/10.1016/j.compositesa.2015.08.038.

[13] Cadu T, Berges M, Sicot O, Person V, Piezel B, Van Schoors L, et al. What are the key parameters to produce a high-grade bio-based composite? Application to flax/epoxy UD laminates produced by thermocompression. Composites Part B: Engineering 2018;150:36–46. https://doi.org/10.1016/j.compositesb.2018.04.059.

[14] Moudood A, Rahman A, Khanlou HM, Hall W, Öchsner A, Francucci G. Environmental effects on the durability and the mechanical performance of flax fiber/bio-epoxy composites. Composites Part B: Engineering 2019;171:284–93. https://doi.org/10.1016/j.compositesb.2019.05.032.

[15] Bar M, Das A, Alagirusamy R. Influence of flax/polypropylene distribution in twistless thermally bonded rovings on their composite properties. Polymer Composites 2019;0. https://doi.org/10.1002/pc.25291.

[16] Pisupati A, Ayadi A, Deléglise-Lagardère M, Park CH. Influence of resin curing cycle on the characterization of the tensile properties of flax fibers by impregnated fiber bundle test. Composites Part A: Applied Science and Manufacturing 2019;126:105572. https://doi.org/10.1016/j.compositesa.2019.105572.

[17] Khalfallah M, Abbès B, Abbès F, Guo YQ, Marcel V, Duval A, et al. Innovative flax tapes reinforced Acrodur biocomposites: A new alternative for automotive applications. Materials & Design 2014;64:116–26. https://doi.org/10.1016/j.matdes.2014.07.029.

[18] Bensadoun F, Vallons KAM, Lessard LB, Verpoest I, Van Vuure AW. Fatigue behaviour assessment of flax–epoxy composites. Composites Part A: Applied Science and Manufacturing 2016;82:253–66. https://doi.org/10.1016/j.compositesa.2015.11.003.

[19] Bensadoun F, Verpoest I, Baets J, Müssig J, Graupner N, Davies P, et al. Impregnated fibre bundle test for natural fibres used in composites. Journal of Reinforced Plastics and Composites 2017;36:942–57. https://doi.org/10.1177/0731684417695461.

[20] Moothoo J, Allaoui S, Ouagne P, Soulat D. A study of the tensile behaviour of flax tows and their potential for composite processing. Materials & Design 2014;55:764–72. https://doi.org/10.1016/j.matdes.2013.10.048.

[21] Shah DU, Schubel PJ, Clifford MJ. Modelling the effect of yarn twist on the tensile strength of unidirectional plant fibre yarn composites. Journal of Composite Materials 2013;47:425–36. https://doi.org/10.1177/0021998312440737.

[22] Madsen B, Thygesen A, Lilholt H. Plant fibre composites – porosity and stiffness. Composites Science and Technology 2009;69:1057–69. https://doi.org/10.1016/j.compscitech.2009.01.016.

[23] Liotier P-J, Pucci MF, Le Duigou A, Kervoelen A, Tirilló J, Sarasini F, et al. Role of interface formation versus fibres properties in the mechanical behaviour of bio-based composites manufactured by Liquid Composite Molding processes. Composites Part B: Engineering 2019;163:86–95. https://doi.org/10.1016/j.compositesb.2018.10.103.

[24] Virk AS, Hall W, Summerscales J. Modulus and strength prediction for natural fibre composites. Materials Science and Technology 2012;28:864–71. https://doi.org/10.1179/1743284712Y.0000000022.

[25] Summerscales J, Virk AS, Hall W. Enhanced rules-of-mixture for natural fibre reinforced polymer matrix (NFRP) composites (comment on Lau et al. in volume 136). Composites Part B: Engineering 2019;160:167–9. https://doi.org/10.1016/j.compositesb.2018.10.021.

[26] Capelle E, Ouagne P, Soulat D, Duriatti D. Complex shape forming of flax woven fabrics: Design of specific blank-holder shapes to prevent defects. Composites Part B: Engineering 2014;62:29–36. https://doi.org/10.1016/j.compositesb.2014.02.007.

[27] Mbakop RS, Lebrun G, Brouillette F. Effect of compaction parameters on preform permeability and mechanical properties of unidirectional flax fiber composites. Composites Part B: Engineering 2019;176:107083. https://doi.org/10.1016/j.compositesb.2019.107083.

[28] Goutianos S, Peijs T. The optimisation of flax fibre yarns for the development of high-performance natural fibre composites. Advanced Composites Letters 2003;12:237–41.

[29] Corbin AC, Soulat D, Ferreira M, Labanieh AR, Gabrion X, Placet V. Multi-scale analysis of flax fibres woven fabrics for composite applications. IOP Conf Ser: Mater Sci Eng 2018;406. https://doi.org/10.1088/1757-899X/406/1/012016.

[30] Omrani F, Wang P, Soulat D, Ferreira M. Mechanical properties of flax-fibre-reinforced preforms and composites: Influence of the type of yarns on multi-scale characterisations. Composites Part A: Applied Science and Manufacturing 2017;93:72–81. https://doi.org/10.1016/j.compositesa.2016.11.013.

[31] Madsen B, Hoffmeyer P, Thomsen AB, Lilholt H. Hemp yarn reinforced composites – I. Yarn characteristics. Composites Part A: Applied Science and Manufacturing 2007;38:2194–203. https://doi.org/10.1016/j.compositesa.2007.06.001.

[32] Ku H, Wang H, Pattarachaiyakoop N, Trada M. A review on the tensile properties of natural fiber reinforced polymer composites. Composites Part B: Engineering 2011;42:856–73. https://doi.org/10.1016/j.compositesb.2011.01.010.

[33] Xie Y, Hill CAS, Xiao Z, Militz H, Mai C. Silane coupling agents used for natural fiber/polymer composites: A review. Composites Part A: Applied Science and Manufacturing 2010;41:806–19. https://doi.org/10.1016/j.compositesa.2010.03.005.

[34] Baley C, Gomina M, Breard J, Bourmaud A, Drapier S, Ferreira M, et al. Specific features of flax fibres used to manufacture composite materials. Int J Mater Form 2018:1–30. https://doi.org/10.1007/s12289-018-1455-y.

[35] Baets J, Plastria D, Ivens J, Verpoest I. Determination of the optimal flax fibre preparation for use in unidirectional flax–epoxy composites. Journal of Reinforced Plastics and Composites 2014;33:493–502. https://doi.org/10.1177/0731684413518620.

[36] Goutianos S, Peijs T, Nystrom B, Skrifvars M. Development of Flax Fibre based Textile Reinforcements for Composite Applications. Appl Compos Mater 2006;13:199–215. https://doi.org/10.1007/s10443-006-9010-2.

[37] Yan L, Chouw N, Jayaraman K. Flax fibre and its composites – A review. Composites Part B: Engineering 2014;56:296–317. https://doi.org/10.1016/j.compositesb.2013.08.014.

[38] Zhang L, Miao M. Commingled natural fibre/polypropylene wrap spun yarns for structured thermoplastic composites. Composites Science and Technology 2010;70:130–5. https://doi.org/10.1016/j.compscitech.2009.09.016.

[39] Baghaei B, Skrifvars M, Salehi M, Bashir T, Rissanen M, Nousiainen P. Novel aligned hemp fibre reinforcement for structural biocomposites: Porosity, water absorption, mechanical performances and viscoelastic behaviour. Composites Part A: Applied Science and Manufacturing 2014;61:1–12. https://doi.org/10.1016/j.compositesa.2014.01.017.

[40] Baghaei B, Skrifvars M. Characterisation of polylactic acid biocomposites made from prepregs composed of woven polylactic acid/hemp–Lyocell hybrid yarn fabrics. Composites Part A: Applied Science and Manufacturing 2016;81:139–44. https://doi.org/10.1016/j.compositesa.2015.10.042.

[41] Baghaei B, Skrifvars M, Berglin L. Characterization of thermoplastic natural fibre composites made from woven hybrid yarn prepregs with different weave pattern. Composites Part A: Applied Science and Manufacturing 2015;76:154–61. https://doi.org/10.1016/j.compositesa.2015.05.029.

[42] Baghaei B, Skrifvars M, Berglin L. Manufacture and characterisation of thermoplastic composites made from PLA/hemp co-wrapped hybrid yarn prepregs. Composites Part A: Applied Science and Manufacturing 2013;50:93–101. https://doi.org/10.1016/j.compositesa.2013.03.012.

[43] AFNOR. NF G07-316 - Textiles - Tests of yarns - Determination of linear density. 1988.

[44] AFNOR. NF G07-079 - Textiles - Testing threads - Determining the twisting of threads by untwisting/retwisting with a double re-test. 2011.

[45] Madsen B, Thygesen A, Lilholt H. Plant fibre composites – porosity and volumetric interaction. Composites Science and Technology 2007;67:1584–600. https://doi.org/10.1016/j.compscitech.2006.07.009.

[46] AFNOR. NF ISO 4602 - Reinforements - Woven fabrics - Determination of number of yarns per unit length of warp and weft. 2011.

[47] Summerscales J, Dissanayake N, Virk A, Hall W. A review of bast fibres and their composites. Part 2 – Composites. Composites Part A: Applied Science and Manufacturing 2010;41:1336–44. https://doi.org/10.1016/j.compositesa.2010.05.020.

[48] Aslan M, Mehmood S, Madsen B. Effect of consolidation pressure on volumetric composition and stiffness of unidirectional flax fibre composites. J Mater Sci 2013;48:3812–24. https://doi.org/10.1007/s10853-013-7182-3.

[49] AFNOR. NF EN ISO 2062 - Textiles - Yarns from packages - Determination of single-end breaking force and elongation at break using constant rate of extension (CRE) tester. 2010.

[50] AFNOR. NF EN 12127 - Textiles - Fabrics - Determination of mass per unit area using small samples. 1998.

[51] AFNOR. NF EN ISO 5084 - Textiles - Determination of thickness of textiles and textile products. 1996.

[52] Ivanov DS, Van Gestel C, Lomov SV, Verpoest I. Local compressibility of draped woven fabrics | Request PDF, Venice: 2012.

[53] Danzi M, Schneeberger C, Ermanni P. A model for the time-dependent compaction response of woven fiber textiles. Composites Part A: Applied Science and Manufacturing 2018;105:180–8. https://doi.org/10.1016/j.compositesa.2017.11.002.

[54] Mbakop RS, Lebrun G, Brouillette F. Experimental analysis of the planar compaction and preforming of unidirectional flax reinforcements using a thin paper or flax mat as binder for the UD fibers. Composites Part A: Applied Science and Manufacturing 2018;109:604–14. https://doi.org/10.1016/j.compositesa.2018.03.036.

[55] ASTM International. ASTM D3039-00 - Test Method for Tensile Properties of Polymer Matrix Composite Materials. 2000. https://doi.org/10.1520/D3039_D3039M-00.

[56] Nguyen QT. Analyse expérimentale et numérique de la compaction des renforts fibreux: Application pour la perméabilité. PhD Thesis. INSA de Lyon, 2011.

[57] Grieser T, Mitschang P. Investigation of the compaction behavior of carbon fiber NCF for continuous preforming processes. Polymer Composites 2017;38:2609–25. https://doi.org/10.1002/pc.23854.

[58] Placet V, Cissé O, Lamine Boubakar M. Nonlinear tensile behaviour of elementary hemp fibres. Part I: Investigation of the possible origins using repeated progressive loading with in situ microscopic observations. Composites Part A: Applied Science and Manufacturing 2014;56:319–27. https://doi.org/10.1016/j.compositesa.2012.11.019.

[59] Berges M, Léger R, Placet V, Person V, Corn S, Gabrion X, et al. Influence of moisture uptake on the static, cyclic and dynamic behaviour of unidirectional flax fibre-reinforced epoxy laminates. Composites Part A: Applied Science and Manufacturing 2016;88:165–77. https://doi.org/10.1016/j.compositesa.2016.05.029.

Table of figures

Table of tables

Declaration of interests

☒ The authors declare that they have no known competing financial interests or personal relationships that could have appeared to influence the work reported in this paper.

☐The authors declare the following financial interests/personal relationships which may be considered as potential competing interests:

Authors' names and affiliations

Anne-Clémence Corbin – ENSAIT, GEMTEX – Laboratoire de Génie et Matériaux Textiles, F-59000, Lille, France

Damien Soulat – ENSAIT, GEMTEX – Laboratoire de Génie et Matériaux Textiles, F-59000, Lille, France

Manuela Ferreira – ENSAIT, GEMTEX – Laboratoire de Génie et Matériaux Textiles, F-59000, Lille, France

Ahmad-Rashed Labanieh – ENSAIT, GEMTEX – Laboratoire de Génie et Matériaux Textiles, F-59000, Lille, France

Xavier Gabrion – FEMTO-ST, CNRS/UFC/ENSMM/UTBM, Besançon - FR

Pierrick Malécot – FEMTO-ST, CNRS/UFC/ENSMM/UTBM, Besançon - FR

Vincent Placet – FEMTO-ST, CNRS/UFC/ENSMM/UTBM, Besançon - FR